Available online at www.sciencedirect.com
SCIENCE DIRECT®
Biochemical and Biophysical Research Communications 330 (2005) 117–122
BBRC
www.elsevier.com/locate/ybbrc

Isolation of wound healing/regeneration genes using restrictive fragment differential display-PCR in MRL/MPJ and C57BL/6 mice

Godfred Masinde [a], Xinmin Li [e], David J. Baylink [a,b], Bay Nguyen [a], Subburaman Mohan [a,b,c,d,*]

[a] *Musculoskeletal Disease Center, JL Pettis VA Medical Center, Loma Linda, CA 92357, USA*
[b] *Department of Medicine, Loma Linda University, Loma Linda, CA 92350, USA*
[c] *Department of Biochemistry, Loma Linda University, Loma Linda, CA 92350, USA*
[d] *Department of Physiology, Loma Linda University, Loma Linda, CA 92350, USA*
[e] *Functional Genomics Facility, The University of Chicago, Chicago, IL 60637, USA*

Received 17 February 2005

Abstract

Wound healing in mammals can take several weeks to months and the process is always accompanied by scar formation. Wound healing mechanisms that mimic regeneration are not found in most mature mammalian tissues. However, the MRL/MPJ (MRL) mouse has the unique capacity to regenerate ear hole wound completely in less than a month. To identify genes involved in wound healing without a scar, we chose to use restriction fragment differential display-PCR to isolate genes differentially expressed in the MRL (good healer) mouse and the C57BL/6 (poor healer) mouse at different stages of wound healing. We identified 36 genes that were differentially expressed in the regenerating tissue of good and poor healer strains of which several genes are also genetically linked to wound healing and thus are potential candidate genes for scarless wound healing.

Keywords: RFDD-PCR; Wound healing; Mice; Regeneration; Gene expression; QTL

Injury is a major contributor to the global burden of disease that occurs both in the battlefield and as accidents in the civilian population. Every day around the world, nearly 16,000 people die from injuries. For every person that dies, several thousands more must endure painful injuries, many of them permanent. Injury is estimated to cost healthcare providers in excess of $500 billion per year in the United States alone [1]. Moreover, there is evidence that incidence of injury is growing [2]. Therefore, there is an urgent need to develop effective strategies to prevent injuries and promote wound healing after injuries.

Injuries in the battlefield or in civilian populations optimally necessitate rapid wound healing with minimal scar formation. However, wound healing of mammalian tissue is a lengthy repair process that only partially recovers the original tissue function with the formation of a scar, a marked contrast to amphibian wound healing wherein wounds are healed rapidly with original architecture and function without scar formation, namely through regeneration [3,4]. Due to the varying rate of wound healing as well as the different degree of functional recovery with regeneration as opposed to wound healing, biomedical scientists have been searching for fast-wound healing/regeneration phenomena in mammals. Several examples of regeneration reminiscent of the tissue regeneration mechanism occurring in amphibians have been found [5]. However, the genetic

* Corresponding author. Fax: +1 909 796 1680.
E-mail address: Subburaman.Mohan@med.va.gov (S. Mohan).

0006-291X/$ - see front matter © 2005 Elsevier Inc. All rights reserved.
doi:10.1016/j.bbrc.2005.02.143

mechanisms regulating fast-healing/regeneration in mammals are not yet known.

Among mammals, the MRL/MPJ (MRL) mouse provides a unique model for studies on the genetic mechanisms that regulate regeneration. This is in contrast to all other mouse strains tested, such as C57BL/6J (B6), which only heals 30% of the ear punch hole with scar tissue after a period of 4 weeks [5,6]. This healing phenotype of the MRL mouse is a heritable quantitative trait with a heritability estimate of 86% [5,6] and thus presents an excellent model system to explore the genetic regulation of fast-wound healing and tissue regeneration in mammals. The overall goal of this study was to identify candidate genes that contribute to fast-wound healing in the MRL mouse by using restrictive fragment differential display (RFDD)-PCR technique [7].

We chose the RFDD-PCR technology to isolate genes that regulate fast-wound healing for several reasons. First, this recently developed, innovative technology overcomes the limitations of standard differential display (i.e., preferential amplification of 3′-ends of the transcripts and a high number of false positives) and has the capacity to not only identify differentially expressed genes, but to also identify the sequence polymorphism within the gene [8,9]. Second, this technology does not require previously constructed cDNA libraries or sequence databases, thus presenting immense advantages when screening for novel therapeutic gene targets. Third, the availability of the entire mouse genome sequence from the public database and available fast-wound healing QTLs further enhance the power of this technology to identify fast-wound healing genes.

To identify the differentially expressed genes between fast and poor healer strains, we compared gene expression at three different stages during wound healing. The first phase (1–7 days) after ear punch represents the inflammatory phase of wound healing that is characterized by the process of hemostasis and initial cleanup [7]. Proteins active at this stage are likely involved in inflammation as well as the early stage of the wound healing process. The second phase (5–20 days), fast-wound healing, involves re-epithelialization, formation of the epidermal/dermal layer, formation of basement membrane and extracellular matrix structure, angiogenesis, formation of hair follicles and sebaceous glands, and chondrogenesis [5,10]. The third phase (>21 days) involves the remodeling stages. In this study, we have identified over 30 genes that are differentially expressed between MRL (fast healer) and B6 (poor healer) mice. We performed real time PCR (RT-PCR) on several genes to confirm results from differential display. In these studies, we have identified some genes with previously known functions in wound healing while others with no prior known function in wound healing.

Materials and methods

Animals. Four-week-old MRL and B6 mice were obtained from The Jackson Laboratories (Bar Harbor, ME) and housed at the Animal Research Facility, JL Pettis VA Medical Center, Loma Linda, CA, under the standard condition of 14 h light, 10 h darkness, ambient temperature of 20 °C, and relative humidity of 30–60%. These two strains were chosen primarily for their extreme differences in wound healing/regeneration [5,10]. At day 25, MRL heals over 90% while B6 heals only 25–30%. In order to evaluate the molecular basis of the fast-healing/regeneration phenotype in MRL mice, we examined differential expression of genes by RFDD-PCR using mRNA extracted from ear tissue. Three 2 mm ear holes were made on 8-week-old female MRL and C57 mice as described previously [5,10]. At different time points after ear punch, mice were euthanized and tissue was collected from the punched ear.

RNA extraction. For differential display, healing tissues were collected at days 7, 14, and 28 after each punch for each strain. For real time PCR, tissues were collected at days 1, 7, and 28 after ear punch. Ear punch tissue collected at day 0 was used for comparison. For each time point, tissues collected from 3 to 5 animals per mouse strain were pooled prior to RNA extraction to increase RNA yield. Two independent RNA pools were used for differential display and three independent RNA pools were used for real time PCR.

Total RNA was extracted from the punched ear tissue from different time points using TRIZOL reagent as detailed in the manufacturer's manual (Qiagen, Valencia, CA). The mRNA was purified from total RNA using the QIAGEN Oligotex mRNA Midi Kit. Approximately 750 ng of mRNA was then used to synthesize cDNA. Phenol/chloroform extraction was performed on the cDNA, followed by endonuclease digestion and ligation of primer adaptors developed by Display Systems Biotech and provided in their display PROFILE kit.

RFDD-PCR. The procedure was carried out as detailed in the protocol from display PROFILE kit developed by Display Systems Biotech (Vista, CA). Briefly, total RNA was reverse transcribed using a random primer and end labeling for radioactive detection was performed using [γ^{33}P]ATP (0.25 mCi) to label a 0-extension primer. This labeled primer was then used to PCR-amplify the cDNA template along with a display PROBE primer selected from the kit. Sixty-four variations of this selection primer are available in the display PROFILE kit. After PCR, 5 μl of the sample was loaded on a 6% urea polyacrylamide gel and run on the genomyx LR DNA sequencer machine. The gel was washed, dried, and autoradiography was performed. The autoradiograph was viewed on a light bank to locate differentially expressed fragments, which were then cut from the gel and re-amplified. PCR products were purified using the QIAQUICK PCR Purification Kit from Qiagen (Qiagen, Valencia, CA).

PCR fragment cloning and sequencing. The differential display fragments were sub-cloned prior to sequencing. A poly(A) tail was added to each of the PCR-amplified product, which was then cloned into a linearized vector provided by Invitrogen's TOPO TA Cloning Kit (Invitrogen, Carlsbad, CA). Chemically competent *Escherichia coli* cells from Invitrogen were used for transformations. Blue/white screening was used to select positive clones. The positive clones were re-amplified using an M13 vector-specific primer. PCR products from the clones were purified using the QIAQUICK PCR Purification Kit from Qiagen. To evaluate the sequence of differentially expressed genes, sequencing reactions were set up using the ABI PRISM Big Dye Terminator version 3 Ready Reaction Cycle Sequencing Kit (Applied Biosystems, Foster City, CA). Sequencing was performed on the ABI PRISM 3100 capillary DNA sequencer (Applied Biosystems). Homology searches for the sequences obtained from bands differentially expressed between MRL and B6 mice were performed using NCBI BLAST.

Real time PCR. Real time PCR (RT-PCR) was performed on several genes to confirm the results of RFDD-PCR. Reverse tran-

scription was carried out in a final volume of 20 μl using Qiagen's Omniscript reverse transcriptase kit according to manufacturer's instructions (Qiagen) with Ambion's Oligo (dt) and ANTI-Rnase. RT-PCR was carried out using SYBR Green QPCR Master Mix kit as described in detail by the manufacturer (Stratagene, La Jolla, CA). Briefly, 1 μl of cDNA at a concentration of 1 μg/μl, and 0.8 μM of each primer (final concentration) to a final volume of 25 μl was prepared. Once the master mix was made, the 25 μl aliquots were transferred into a MicroAmp Optical 96-well reaction plate (Applied Biosystems), vortexed, and sealed with an optical adhesive cover (Applied Biosystems). The amplification was performed in an ABI Prism 7900 HT sequence detection system (Applied Biosystems) under the following cycling conditions: initial activation at 95 °C for 10 min, then 40 cycles at 95 °C for 15 s and 60 °C for 1 min. Product specificity was checked by including a dissociation stage according to the manufacturer's instructions (Applied Biosystems). GAPDH was used as an internal control. Delta C_T (C_T value for gene of interest minus C_T value for GAPDH housekeeping gene) values were determined using the software provided by Applied Biosystems. Delta C_T for days 1, 7, and 28 were compared with day 0 control tissue to calculate fold changes in gene expression.

Results

Restrictive fragment differential display (RFDD-PCR)

RFDD-PCR technique relates gene expression to the concentration of the corresponding cDNA amplified by PCR. Double-stranded cDNA was amplified from total RNA and digested with *Taq*1 restriction enzyme. After digestion and adaptor ligation, we amplified the template with 0-extension primer combined with a 3-extension primer. Therefore, each PCR primer amplified only a specific subset of the cDNA fragments that had a specific 3 base sequence upstream of *Taq*1 restriction site. We amplified all subsets using over 101 primers as it gives a complete cross-section of the expressed sequences. The PCR products were visualized by labeling of the 0-extension primer and exposing the gel to an X-ray film and the bands were cut out and extracted from the gel, cloned, and sequenced.

Sequence homology of over-expressed fragments

RNA from ear punch holes of 3–5 animals was pooled and two individual pools from each mouse strain were used for RFDD-PCR. Those bands that were differentially expressed in the independent pools were considered positive and were used for subsequent cloning and sequencing. PCR was performed on isolated bands that were subsequently cloned and sequenced. Homology search between the cloned sequences and known genes was performed using the NCBI Blast tool. The sequences with over 90% homology with known genes were selected for further analysis for known functions in wound healing/regeneration. Following these criteria, 36 genes were identified that were differentially expressed in the healing tissue of MRL and B6 mice.

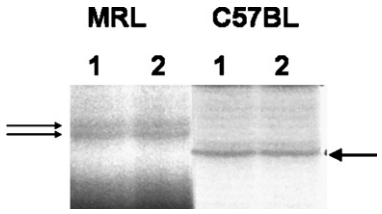

Fig. 1. A representative portion of autoradiograph gel picture showing differentially displayed bands for RNA pools from MRL and B6 mice at day 7. The arrows show differentially displayed bands for RNA samples between MRL and B6 mice.

Fig. 1 shows an example of differential display bands obtained for two independent RNA pools for MRL and B6 mice at day 7.

Table 1 shows the list of 36 genes differentially expressed in MRL and B6. There are about 6 genes that have a documented role in wound healing and the remaining 30 genes have no known role in wound healing. The majority of the 36 genes are found to be located in the soft tissue regeneration (STR) QTL regions and some genes are expressed in regenerating ear tissue of MRL, but not B6 mice. The largest group of those genes plays a role in protein biosynthesis (ribosomal protein L7a, ETS-related transcription factor, mouse acidic ribosomal phosphoprotein, mouse ribosomal protein S9, mouse similar to ribosomal protein S9, and mouse ribosomal protein L7a). The remaining genes have established roles in extracellular cytoskeletal organization and biogenesis (mouse decorin), aerobic respiration (mouse cytochrome *C* oxidase), regulation of translation (elongation factor 1α1), intermediate filament-based process (mouse vimentin), and epidermal differentiation and cellular morphogenesis (mouse keratin 1–14). Some genes play more than one role, for example, mouse ETS-related transcription factor has a role in translational termination, nascent polypeptide association; ethylene mediated signaling pathway and defense response to pathogens.

Real time PCR

In order to validate the results from RFDD-PCR, real time polymerase chain reaction (RT-PCR) was used to evaluate the differences in expression levels of some of the genes identified. Fig. 2 shows data using RT-PCR, which confirmed the results from RFDD-PCR. The genes tested by RT-PCR were up regulated more in MRL than in B6 at day 7 after ear punch as indicated by the RFDD-PCR method.

Discussion

The MRL mouse has the unique capability of healing a through and through ear punch hole faster than

Table 1
Genes that were differentially expressed in the regenerating tissues between MRL and C57BL/6 mice at different time points

Gene sequence identified	Ontology	Time point (Days)	Homo score	# clone sequenced	Chr. #	Increase MRL or B6
Mouse Decorin (DCN)	Extracellular matrix org. and biogenesis	D7	517/522	1	10	B6
Mouse DEAD/H	Pre-mRNA splicing, mRNA translation, and RNA stability	D7	270/285	1	9	MRL
Ribosomal Protein L7a (Rp17a)	Protein biosynthesis	D7	221/224	1	1	MRL
Mouse Vimentin (Vim)	Intermediate filament-based process	D7	293/295	1	2	MRL
Mouse Transcription Repressor	Unknown	D7	174/174	1	3	MRL
Mouse Proteasome (prosome, macropain)	Transcription, vesicular trafficking	D7	298/299	1	3	MRL
Mouse Nascent Polypeptide Associated Complex Alpha (NACA)	DNA metabolism, DNA topological change	D7	293/296	1	10	MRL
Mouse ETS-Related Transcription Factor (Erf1)	Protein biosynthesis, ranslational termination nascent, polypeptide association, ethylene-mediated signaling, pathway defense response to pathogen	D7	274/274	1	17	MRL
Mouse Cytochrome *C* Oxidase (Cox)	Electron transport, aerobic respiration, energy pathways	D7	253/257	1	9	B6
Mouse Baculoviral IAP	Unknown	D28	499/511	1	13	B6
Mouse Chromosome 1 Clone	Unknown	D28	499/511	1	9	B6
Mouse Neuronal Apoptosis Inhibitory Protein 6	Unknown	D28	510/521	1	13	MRL
Elongation Factor 1-Alpha 1 (EF1-alpha 1)	Regulation of transcription	D7	599/603	1	16	MRL
Mouse 0 Day Neonate Head cDNA	Unknown	D7	598/616	1	15	MRL
Mouse Similar to Homerin	Keratinization of epidermal tissues	D7	512/519	1	3	MRL
Mouse Similar to Keratin 14 (Krt-14)	Cytoskeleton org. and biogenesis, epidermal differentiation, cellular morphogenesis	D7	454/457	1	11	MRL
Mouse mRNA for 28 kDa Interferon Alpha responsive protein (1frg28 gene)	Unknown	D7	422/431	1	16	MRL
Mouse Keratin Complex 1, Acidic, Gene 14 (Krt1–14)	Cytoskeleton org. and biogenesis, epidermal differentiation, cellular morphogenesis	D7	444/448	2	11	MRL
Human Keratin 17 (Krt-17)	Cellular morphogenesis	D7	410/447	2	11	MRL
Cytochrome *B* (cytb)	Mitochondrial electron transport, ubiquinol to cytochrome	D7	449/457	1	9	MRL
Mouse mRNA for RCK	Post-transcriptional regulation of gene expression	D7	270/285	1	11	MRL
Mouse Similar to Retrovirus-Related POL Polyprotein	Unknown	D14	232/243	2	9	MRL
Mouse Similar to Hypothetical Protein ORF-1137	Unknown	D14	232/243	4	12	MRL
Mouse Serine Palmitoyltransferase (Sptlc)	Metabolism, biosynthesis	D7	427/428	1	12	MRL
Human Serine/Threonine Protein Kinase	Unknown	D7	181/185	2	12	B6
Mouse Acidic Ribosomal Phosphoprotein PO (Arbp)	Protein biosynthesis, translation elongation	D28	212/213	1	5	B6
Mouse Ribosomal Protein S18 (Rps18)	Protein biosynthesis, translational initiation, ribosome biogenesis	D28	204/204	1	17	B6
Mouse Similar to Ribosomal Protein S9 (Rps9)	Protein biosynthesis	D14	397/398	1		B6
Mouse Nascent Polypeptide-Associated Complex Alpha Polypeptide (Naca)	DNA metabolism, DNA topological change	D14	332/335	1	10	B6
Mouse RecQ Protein-Like 5 (Recq15)	DNA metabolism, DNA repair	D14	281/289	1		B6

Table 1 (*continued*)

Gene sequence identified	Ontology	Time point (Days)	Homo score	# clone sequenced	Chr. #	Increase MRL or B6
Antigen LEC-A	Unknown	D14	414/418	1	16	MRL
Mouse CNR Gene for Cadherin-Related Neuronal Receptor	Unknown	D14	197/197	1		B6
Mouse Cytochrome *C* Oxidase, Subunit Va (cox5)	Electron transport, aerobic respiration, energy pathways	D28	139/156	1	9	B6
Mouse Ribosomal Protein L7a (Rps7a)	Protein biosynthesis	D28	224/224	2		B6
Mouse mRNA for suppressor of Actin Mutations (SAC1 gene)	Dorsal closure, phosphoinositide metabolism, dephosphorylation	D28	66/66	4	9	B6
Mouse Poly A Binding Protein, Cytoplasmic 1 (Pabpn1)	mRNA polyadenylation	D28	181/182	1		B6

Homology score for the various genes identified and their chromosomal location are also shown. Some of the genes were identified using different primers. Of the 36 identified genes, 21 were expressed more in MRL and 15 were expressed more in B6 mice.

other mice strains and without a scar (regeneration) [5,10], although the mechanism by which the MRL mouse regenerates the ear hole injury is not known.

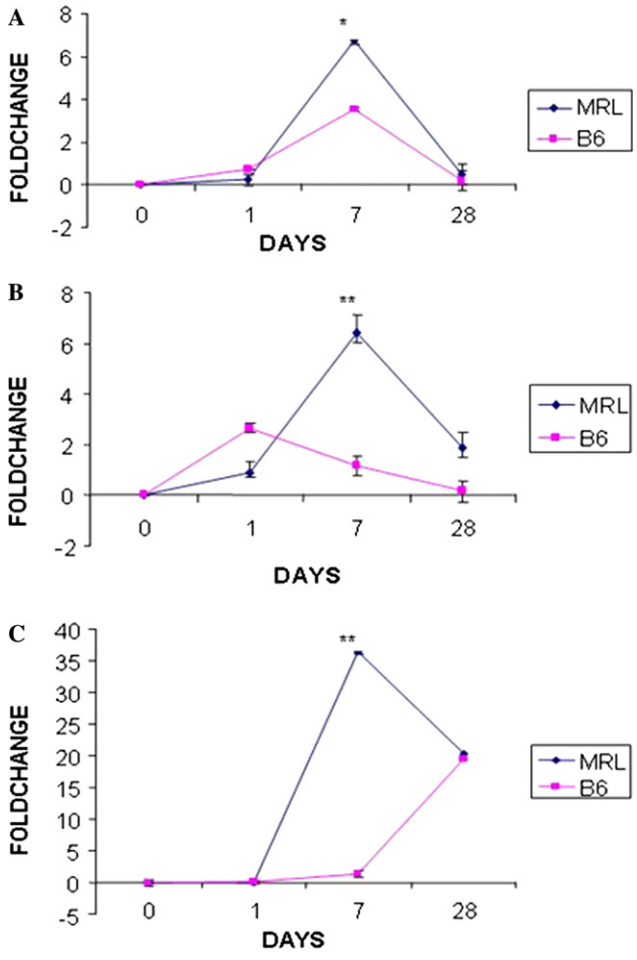

Fig. 2. Shows real time PCR for vimentin (A), elongation factor α1 (B), and Krt1–14 (C) using RNA extracted from healing tissue of MRL and B6 mice at days 1, 7, and 28. Values are means ± SEM of three different RNA pools per time point. $*P < 0.01$ versus B6. $**P < 0.001$ versus B6. GAPDH was used as an internal control. Gene expression in fold changes was calculated by comparing delta CT for each time point with time 0 for a given mouse strain.

In contrast, B6 mice heal less than 25% in 4 weeks but with a scar [11,12]. In this study, we have used RFDD-PCR to identify genes that are differentially expressed with healing tissues, and good and poor healer strains of mice. The identification of several genes which have not been previously established to play a role in wound healing provides evidence that wound healing is a complex process.

We believe that the differentially expressed genes identified by RFDD-PCR are potential candidate genes for wound healing for a number of reasons. First, we discovered genes in this study that have been previously implicated in wound healing. For example, we found that vimentin is highly expressed in the regenerating tissue of MRL but not B6 mice. Vimentin, a major structural component of intermediate filament in cells of mesenchymal origin, has been considered as provider of an intracellular scaffold that supplies cells strength and tissue integrity. Recent studies using mice lacking vimentin have provided evidence that in both embryonic and adult situations, vimentin is necessary for the connective tissue component of repair [13]. Furthermore, it has recently been found that skin healing is impaired in mice lacking vimentin [14]. In addition to vimentin, we have also found that Krt1–14 (keratin complex) was expressed in high levels in the regenerating ear tissue of MRL but not in B6 mice. Because MRL but not B6 mice exhibit scarless ear regeneration, it is not surprising that keratin complex gene is differentially expressed in the regenerating ear of MRL and B6 mice. These data provide validation that RFDD-PCR technology is useful to identify candidate genes that contribute to differences in wound healing between MRL and B6 mice.

Second, many of the differentially expressed genes identified by RFDD-PCR are located within the QTL regions that have been identified using various crosses of good and poor healer mouse strains. In this regard, we and others have identified more than 15 QTLs using F2 population generated from good healer MRL and poor

healing B6 or SJL mice [5,10]. These soft tissue regeneration QTLs are located in a number of chromosomes. If the genes identified by RFDD-PCR are in fact candidate genes for wound healing, we would expect some of the genes to be located within the soft tissue regeneration QTL regions. This is, in fact, true. Table 1 shows that a number of differentially expressed genes are located in chromosome 9 which contains a major QTL for soft tissue regeneration. The finding that the differentially expressed genes are located within the QTL regions provides another validation for the utility of RFDD-PCR to identify wound healing candidate genes.

Third, we have validated the differential expression data obtained using RFDD-PCR using real time PCR for some of the genes. For example, vimentin, elongation factor 1α1, and keratin complex 1 gene were identified as differentially expressed genes by RFDD-PCR using RNA extracted from MRL and B6 mice at day 7 after ear punching. Accordingly, real time PCR analysis showed that the expression levels of these three genes were indeed significantly elevated in the regenerating tissue of MRL mice compared to B6 mice at day 7 (Fig. 2). These data provide further experimental evidence on the reliability of RFDD-PCR to identify differentially expressed genes as candidate genes for wound healing.

In our study, we also found that a number of genes which have not been previously implicated in wound healing are differentially expressed in the wound healing tissue of MRL and B6 mice. In this regard, a number of genes related to protein synthesis and energy metabolism are differentially expressed in the healing tissue of MRL and B6 mice. Furthermore, genes involved in transcriptional regulation and mRNA stability are also differentially expressed in the regenerating tissue of MRL and B6 mice. Because many of these genes are located within the QTL regions previously identified, it is likely that some of these genes are potential candidate genes for future studies.

In conclusion, we have identified over 30 genes differentially expressed in the MRL or B6 mice that include those that are known to regulate wound healing and those with no known function in wound healing. These genes belong to different ontologies that may be involved in wound healing/regeneration. We have also identified several genes that are within the wound healing QTL regions. The identification of genes that are differentially expressed and also genetically linked to wound healing provides a framework for future identification of wound healing genes.

Acknowledgments

The research reported in this manuscript was supported by the Department of the Army Cooperative Agreement Number (DAMD 17-97-2-7016). The views and content of the information do not necessarily reflect the position or the policy of the government or NMTB, and that no official endorsement should be inferred. The authors thank Debleena Sinha, Anil Kapoor, Nia Wedhas, Heather Davidson, and Melanie Hamilton-Ulland for their excellent technical support, and Shelley Levtzow and Sean Belcher for secretarial help. All work was performed at the Jerry L. Pettis VA Medical Research Facilities in Loma Linda, CA.

References

[1] C.J. Murray, A.D. Lopez, Alternative projections of mortality and disability by cause 1990–2020: global burden of disease study, Lancet 349 (1997) 1498–1504.
[2] R. Goss, Getting to mammalian wound repair and amphibian limb regeneration: a mechanistic link in the early events, Wound Rep. Reg. 4 (1996) 190–202.
[3] L.D. Clark, R.K. Clark, E. Heber-Katz, A new murine model for mammalian wound repair and regeneration, Clin. Immunol. Immunopathol. 88 (1998) 35–45.
[4] G.K. Michalopoulos, M.C. DeFrances, Liver regeneration, Science 276 (1997) 60–66.
[5] G.L. Masinde, X. Li, W. Gu, H. Davidson, S. Mohan, D.J. Baylink, Identification of wound healing/regeneration quantitative trait loci (QTL) at multiple time points that explain seventy percent of variance in (MRL/MpJ and SJL/J) mice F2 population, Genome Res. 11 (2001) 2027–2033.
[6] A. Fisher, H. Saedler, G. Theissen, Restriction fragment length polymorphism-coupled domain-directed differential display:a highly efficient technique for expression analysis of multigene families, Proc. Natl. Acad. Sci. USA 92 (1995) 5331–5335.
[7] E. Heber-Katz, The regenerating mouse ear, Semin. Cell Dev. Biol. 10 (1999) 415–419.
[8] M. Monticone, Y. Liu, L. Tonachini, M. Mastrogiacomo, S. Parodi, R. Quarto, R. Cancedda, P. Castagnola, Gene expression profile of human bone marrow stromal cells determined by restriction fragment differential display analysis, J. Cell. Biochem. 92 (2004) 733–744.
[9] M.L. Wrang, F. Moller, C.W. Alsbo, N.H. Diemer, Changes in gene expression following induction of ischemic tolerance in rat brain: detection and verification, J. Neurosci. Res. 65 (2001) 54–58.
[10] B.A. McBrearty, L.D. Clark, X.M. Zhang, E.P. Blankenhorn, E. Heber-Katz, Genetic analysis of a mammalian wound-healing trait, Proc. Natl. Acad. Sci. USA 95 (1998) 11792–11797.
[11] E.P. Blankenhorn, S. Troutman, L.D. Clark, X.M. Zhang, P. Chen, E. Heber-Katz, Sexually dimorphic genes regulate healing and regeneration in MRL mice, Mamm. Genome 14 (2003) 250–260.
[12] X. Li, W. Gu, G. Masinde, M. Hamilton-Ulland, S. Xu, S. Mohan, D.J. Baylink, Genetic control of the rate of wound healing in mice, Heredity 86 (2001) 668–674.
[13] E. Colucci-Guyon, Y.R.M. Gimenez, T. Maurice, C. Babinet, A. Privat, Cerebellar defect and impaired motor coordination in mice lacking vimentin, Glia 25 (1999) 33–43.
[14] B. Eckes, E. Colucci-Guyon, H. Smola, S. Nodder, C. Babinet, T. Krieg, P. Martin, Impaired wound healing in embryonic and adult mice lacking vimentin, J. Cell Sci. 113 (2000) 2455–2462.